

## Synthesis, characterization and anticancer activity of NiO nanoparticles from a Ni(II) complex derived from chitosan and pyridine derivative

M. S. Al-Fakeh<sup>1,2</sup>

<sup>1</sup>Department of Chemistry, College of Science, Qassim University, Buraidah 51452, Saudi Arabia

<sup>2</sup> Taiz University, Taiz, Republic of Yemen

Received: December 31 2020; Revised: June 28, 2021

Synthesis of NiO nanoparticles (NPs) by a calcination method is the approach used in this article. Materials utilized were nickel chloride hexahydrate, chitosan (CS) and 2-aminopyridine (2-AMPY) ligands for the preparation of the nickel(II) complex, [Ni(CS)(2-AMPY)(H<sub>2</sub>O)<sub>3</sub>]. NPs properties were identified by Fourier transform infrared (FTIR) spectroscopy, UV, TG, X-ray powder diffraction and scanning electron microscopy (SEM). The results obtained prove the presence of nickel oxide NPs produced during calcination. Finally, the anti-cancer activity of the nickel oxide NPs was studied. The cytotoxic effectiveness of the NiO NPs was examined in cultured human breast cancer cells. The results of the present study indicate that the NiO NPs could increase the permeability of cancer cell wall.

**Keywords:** Mixed-ligand complex, NiO nanoparticles, XRD, Anti-cancer activity.

### INTRODUCTION

Currently, nanomaterials such as nanoparticles (NPs), nanotubes and nanowires exhibit electronic, magnetic, mechanical, thermal, and catalytic properties, and are used in chemical reduction, photo-reduction, electrochemical reduction, spray pyrolysis, laser and ablation methods [1-5]. Metal oxide nanoparticles (MONPS) preparation and properties constitute a major research field in materials chemistry; mostly relevant is the use of nanoparticles in nanotechnology applications, because metal particles sized in the nanometer scale (1-100 nm) possess specific physical, chemical and biological properties [6-11]. The biological activity of these NPs depends on their stability, concentration and size when added to the microbe's growth medium, so this provides more confinement time for interaction of microbes with nano-particles. Highly ionic nickel oxide NPs may be particularly important antimicrobial, antifungal and anticancer agents as they can be synthesized with extremely high surface areas and unusual crystal shapes [12, 13]. Chitosan (CS), the product of N deacetylation of chitin widely spread in shell fish and cell walls of plants or fungi, is an important renewable natural resource. It is also well-known that chitosan has antifungal activity, biocompatibility and biodegradation due to its chemical and physical properties, as well as unusual biological activity, which have been used in food, catalysis, material and pharmaceutical applications [14-17]. Moreover, the complex-forming ability of pyridine and its derivatives with transition metal ions is well-known, 2-aminopyridine acting as a monodentate

ligand through its pyridine N-atom [18]. Thus, the chemistry of nickel(II) mononuclear compounds with O- and N-containing groups, especially pyridine ligands, has been widely studied [19, 20]. There are several chemical or mechanical processes developed for synthesizing crystalline metal oxide powders in nanoscale dimensions. The purpose of this work is the synthesis and characterization of a new complex derived from chitosan, a pyridine derivative and nickel(II). The resulting mixed-ligand complex was used as a precursor for preparation of NiO nanoparticles.

### EXPERIMENTAL

#### *Material and physical measurements*

Chitosan with more than 90% degree of deacetylation and 2-aminopyridine were purchased from Sinopharm chemical reagent Co., Ltd, China and Sigma-Aldrich, respectively. All materials and solvents utilized were commercially available and employed as received without further purification.

The elemental analysis (carbon, hydrogen and nitrogen) was performed using Analytischer Funktionstest Vario El Fab-Nr.11982027 elemental analyzer. For more details of the other physical measurements see [5]. The cytotoxic activity of the synthesized compound was studied at the National Research Center, Cairo, Egypt.

#### *Cytotoxic activity*

*Materials of the cell lines assay.* Cell culture of HCT-116 (human colorectal carcinoma) and MCF-7 (human breast adenocarcinoma) cell lines were purchased from the American Type Culture

\*To whom all correspondence should be sent:  
E-mail: [m.alfakehqu.edu.sa](mailto:m.alfakehqu.edu.sa)

Collection (Rockville, MD, USA) and maintained in Dulbecco's Modified Eagle Medium (DMEM) which was supplemented with 10% heat-inactivated fetal bovine serum (FBS), 100 U/mL penicillin, and 100 U/mL streptomycin. The cells were grown at 37 °C in a humidified atmosphere of 5% CO<sub>2</sub>.

**MTT cytotoxic assay.** The cytotoxic activities against HCT-116 and MCF-7 human cancer cell lines were estimated using the 3-[4,5-dimethyl-2-thiazolyl]-2,5-diphenyl-2H-tetrazolium bromide (MTT) assay which is based on the reduction of the tetrazolium salt by mitochondrial dehydrogenases in viable cells [21, 22]. Cells were dispensed in a 96-well sterile microplate (1×10<sup>4</sup> cells/well) and incubated at 37 °C with a series of different concentrations of each tested compound or doxorubicin (positive control) in DMSO for 48 h in a serum-free medium prior to the MTT assay. After incubation, the media were carefully removed, 40 μL of MTT (2.5 mg/mL) were added to each well and then incubated for additional 4 h. The purple formazan dye crystals were solubilized by the addition of 200 μL of DMSO. The absorbance was measured at 570 nm using a Spectra Max Paradigm Multi-Mode microplate reader. The relative cell viability was expressed as the mean percentage of viable cells compared to the untreated control cells.

#### Synthesis of [Ni(CS)(2-AMPY)(H<sub>2</sub>O)<sub>3</sub>]<sub>n</sub>

Chitosan (1 g, 0.5 mmol) was added to 60 ml of distilled water containing 0.4 ml of acetic acid at room temperature and stirred until the chitosan ligand was dissolved. Then 25 ml of NiCl<sub>2</sub>·6H<sub>2</sub>O (1.47 g, 0.6 mmol) was added into the dissolved chitosan. The solution mixture was then stirred for about 15 min and an ethanolic solution of 2-aminopyridine (0.58 g, 0.5 mmol) was added to the mixture. The solution mixture was heated on a water bath for about 50 min whereupon a light-green precipitate was formed which was filtered and washed with ethanol and dried. Analysis for C<sub>11</sub>H<sub>23</sub>N<sub>3</sub>NiO<sub>7</sub>: Theoretical value: C, 35.89; H, 6.31;

N, 11.41. Experimental values: C, 34.96; H, 6.22; N, 11.08, melting point 186 °C.

#### Formation of NiO nanoparticles

By calcining the synthesized complex in air at 450 °C with a calcination time of 4 h NiO nanoparticles were obtained.

#### RESULTS AND DISCUSSION

The reaction of nickel(II) with chitosan and 2-aminopyridine yields a mixed-ligand complex. This Ni(II) complex is stable in air and insoluble in common organic solvents, but partially soluble in dimethyl sulfoxide (DMSO).

#### Fourier transform infrared spectroscopy (FT-IR)

Figure 1 shows the FT-IR spectrum of the synthesized Ni(II) complex. The strong and broad band at 3424 cm<sup>-1</sup> is attributed to OH asymmetrical stretching vibration and amino (NH<sub>2</sub>) stretching vibrations; the band at 1418 cm<sup>-1</sup> is related to -CH<sub>2</sub> bending, and the absorption band at 1070 cm<sup>-1</sup> is due to C-O-C stretching vibration in glucosidic linkage [23]. The FT-IR spectrum of the nickel(II) complex shows at 3434 cm<sup>-1</sup> -OH, -NH<sub>2</sub>; at 2928 cm<sup>-1</sup> and 2862 cm<sup>-1</sup> -C-H stretching; at 1632 cm<sup>-1</sup> -C=O, amide; 1460 cm<sup>-1</sup> (-CH<sub>2</sub>-N) coupled with 1380 cm<sup>-1</sup> (-N-H); 1155 cm<sup>-1</sup> (skeleton C-O and -C-O-C); at 888 cm<sup>-1</sup> C-O-C bridge, as well as glucosidic linkage. All these vibrational peaks are characteristic for chitosan. On the other hand, for the 2-AMPY, the absorption peaks in the area around 3365 and 3473 cm<sup>-1</sup> indicate the existence of amino (NH<sub>2</sub>) group in the nickel(II) complex [24]. These peaks also indicate that the amino N-atom does not participate in the bonding [25]. 2-Aminopyridine displays two bands at 904 and 1468 cm<sup>-1</sup> which can be referred to ν(C-N) ring vibrations [26]. Finally, the bands at 576 and 528 cm<sup>-1</sup> are attributed to (Ni-N-) and that at 425 cm<sup>-1</sup> to (Ni-O).

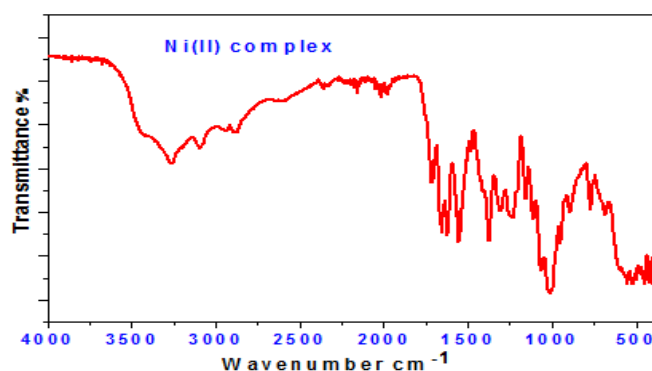
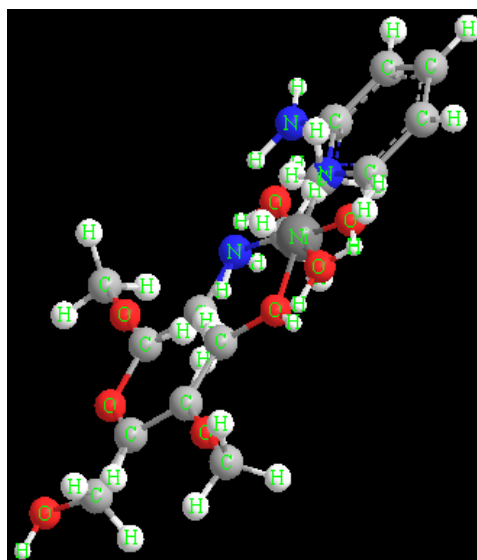


Figure 1. FT-IR spectrum of the Ni(II) complex.

*Electronic spectra*

Electronic spectra of Ni(II) mixed ligand complex and nickel oxide nanoparticles recorded in the 200-900 nm region in dimethyl sulfoxide (DMSO) solution are shown in Fig. 2. The spectrum of the Ni(II) complex shows two distinct bands at 235 and 434 nm which are referred to ( $\pi \rightarrow \pi^*$ ) and ( $n \rightarrow \pi^*$ ) transitions within the 2-ampy and chitosan ligands, respectively [27, 28]. The structure of the nickel complex can be assumed as follows:



(b)



(c)

(a)

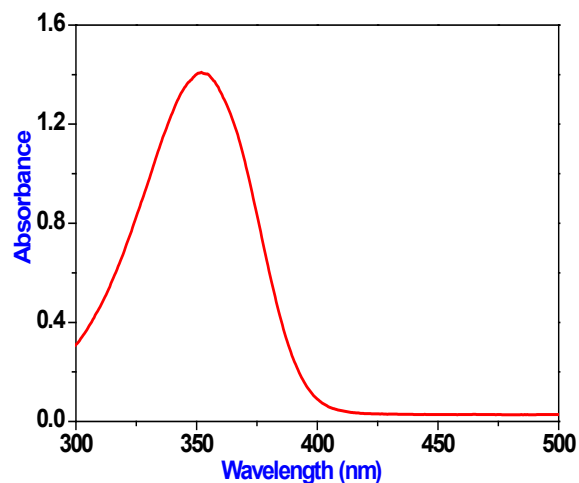
**Figure 2.** (a) Structure of the Ni(II) complex, (b) Estimation view of coordination round Ni(II), (c) DFT (HOMO-LUMO) molecular orbital plots for frontier molecular orbitals of NiO.

Figure 2 (c) shows that the charges being carried by the atoms, cause a dipole moment of 2.9178 debye and total energy of 1575.6 a.u. Fig. 3. displays the UV-vis absorption spectrum of NiO nanoparticles. It is apparent that the spectrum exhibits a band absorption edge at 348 nm [29].

*Thermal analysis studies*

The thermal decomposition of the nickel(II) compound was inspected from ambient temperature to 650 °C. The thermogram of this complex displays four decomposition steps (Fig. 4), at 28-90, 92-250, 252-390 and 392-650 °C. The first step corresponds to the detachment of the coordinated water (calc. 14.08 %, found 13.87 %). The DTG curve of this step shows a minimum at 56 °C and an endothermic peak at 58 °C in the DTA trace. The mass loss in the second step indicates the release of 2-aminopyridine ligand (calc. 24.50 %, found 24.26 %) (DTG peaks

at 225 °C) with a broad exothermic peak in the DTA trace at 227 °C.



**Figure 3.** UV-vis absorption spectrum of the NiO nanoparticles.

The third and fourth steps identify the decomposition of the organic ligands (DTG peaks at 350 and 475 °C) with two exothermic peaks in the

DTA curve at 352 and 477 °C. The final product was identified as nickel oxide (calc. 19.45 %, found 18.92 %).

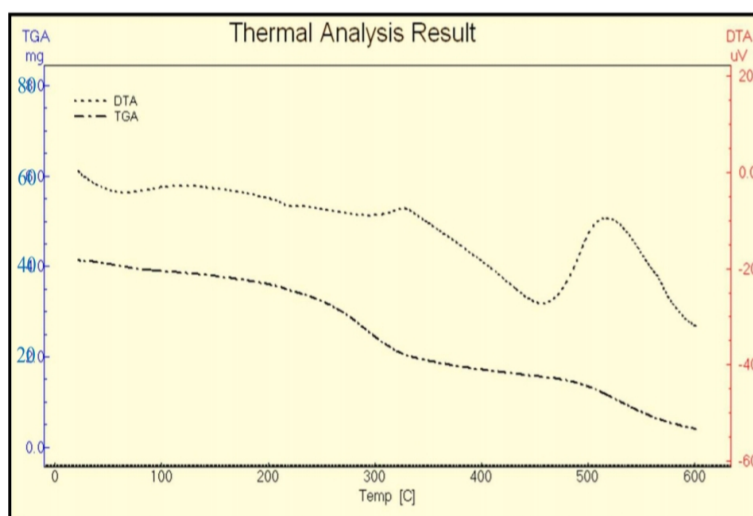


Figure 4. TGA and DTA curves of the Ni(II) complex.

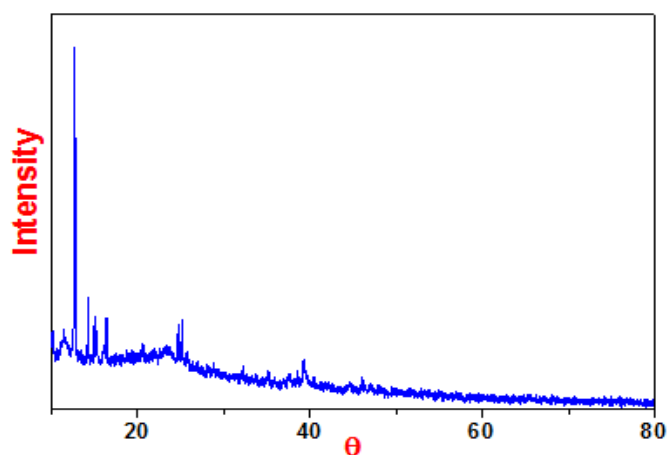


Figure 5. X-ray powder diffraction pattern of the nickel(II) complex.

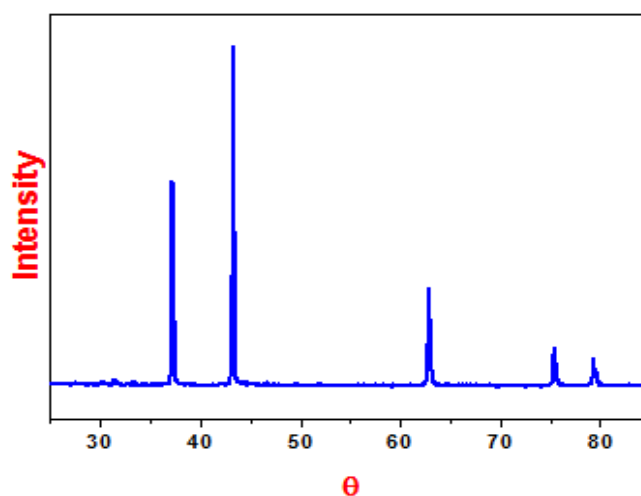
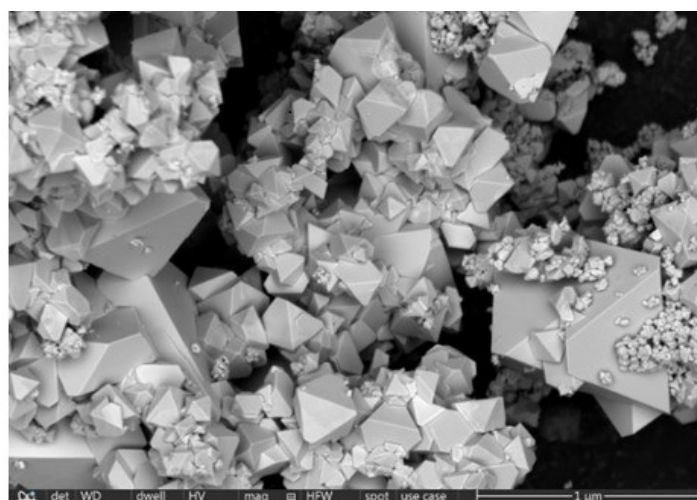


Figure 6. X-ray powder diffraction pattern of the nickel oxide nanoparticles.

**Table 1.** XRD crystal data of the compounds.

| Parameters                            | Ni(II) compound   | NiO       |
|---------------------------------------|---|-----------|
| Empirical formula                     | C <sub>11</sub> H <sub>23</sub> NiN <sub>3</sub> O <sub>8</sub> | NiO       |
| Formula weight                        | 384.00  | 74.68     |
| Crystal system                        | Triclinic   | Hexagonal |
| a (Å)                                 | 8.02  | 2.95      |
| b (Å)                                 | 10.25   | 2.95      |
| c (Å)                                 | 2.74  | 7.23      |
| α (°)                                 | 94.56   | 90.00     |
| β (°)                                 | 99.21   | 90.00     |
| γ (°)                                 | 103.42  | 120.00    |
| Volume of unit cell (Å <sup>3</sup> ) | 214.83  | 54.67     |
| Particle size (nm)                    | 156   | 74        |



**Figure 7.** SEM of NiO nanoparticles.

#### *Scanning electron microscopy (SEM)*

The scanning electron micrograph of nickel oxide NPs is shown in Fig. 7. SEM is perfect to illustrate the NiO nanoparticles morphology, and clearly shows the formation of NiO nanoparticles in the form of hexagonal groupings.

#### *Cytotoxicity studies*

The suggested inducement of intracellular oxidative stress is to be a key event in the toxicity mechanisms of metal oxide nanoparticles (MONPs) such as NiO NPs. The oxide nanoparticles enter inside the cell; this nanomaterial may induce intracellular oxidative stress by annoying the balance between oxidant and antioxidant reactions. On the other hand, the photo-catalysis appears to be

the more important anti-cancer mechanism. Reactive oxygen species (ROS) produced on the surface of these nanoparticles in the presence of light cause an oxidative stress in the microbial cell. This eventually leads to the death of the cell. Also the generated NPs can penetrate into the cell membrane and kill the microbes [30]. From the oxidative stress produced by exposure to nanomaterials an increase of the cytosolic Ca<sup>2+</sup> concentration may be catalyzed or may cause the translocation of transcription factors to the nucleus, which arrange pro-inflammatory genes. Alternatively, overriding oxidative stress may also adjust lipids, proteins and nucleic acids, which further stimulates the anti-oxidant defense system or even leads to cell death [31]. The cytotoxic effect of the NiO NPs was examined on cultured human breast cancer cells by exposing cells for 72 h to the

medium containing the nickel oxide nanoparticles at 5-100 µg/ml concentration. In relation to cell death, a minimum concentration for NiO NPs is well enough to induce it. The micro-organisms carry a negative charge while metal oxides carry a positive charge [32, 33]. This causes electromagnetic attraction between the microbe and the treated surface of nanoparticles. When the metal oxide NPs approach the microbes, the latter oxidize and die immediately. The cytotoxic effect of the NiO nanoparticles at 100 µM on lung adenocarcinoma A549, and prostate cancer (PC3) human tumor cell lines and RPE1 human normal cell line, was 39%, 0% and 41% for A-549, PC3 and RPE1 respectively, compared to doxorubicin taken as 100%. The XRD and SEM demonstrated the decrease in particle size for NiO NPs, which increases the release of Ni<sup>2+</sup> ions. The more Ni<sup>2+</sup> ions contact the cell membrane, the higher damage is caused to cancer cell membrane.

### CONCLUSIONS

NiO nanopowder was successfully synthesized using nickel chloride hexahydrate and two organic ligands, chitosan (CS) and 2-aminopyridine (2-AMPY) to prepare a Ni(II) complex which was subsequently calcined.

The X-ray pattern shows that all peaks can be well attributed to the phase of NiO. The SEM micrograph manifested that there are some micropores between the nanocrystals for the sample calcined at 450 °C for 4 h. The majority of obtained NiO nanopowders had an average particle size less than 74 nm. The cytotoxic effect of the nickel oxide NPs was examined on cultured human breast cancer cells by exposing cells for 72 h. NiO NPs showed anticancer activity.

### REFERENCES

1. O. Długosz, M. Banach, *Colloids and Surfaces A: Physicochemical and Engineering Aspects*, **5** (12), 606 (2020).
2. M. C. Higgins, S. Ghobadi, J.V. Rojas, C. E. Castano, *Applied Surface Science*, **12** (4), 146313 (2020).
3. Q. Li, L.-S. Wang, B.-Y. Hu, C. Yang, L. Zhou, L. Zhang, *Materials Letters*, **61** (8-9), 1615 (2007).
4. X. Xin, Z. Lu, B. Zhou, *Journal of Alloys and Compounds*, **427**(1-2), 251 (2007).
5. M. S. Al-Fakeh, F. M. Alminderej, *International Journal of ChemTech Research*, **11**(5), 442 (2018).
6. Y. Wu, Y. He, T. Wu, T. Chen, W. Weng, H. Wan, *Materials Letters*, **61** (14-15), 3174 (2007).
7. N. Acacia, F. Barreca, E. Barletta, D. Spadaro, G. Currò, F. Neri, *Appl. Surf. Sci.*, **256**, 6918 (2010).
8. Y. B. M. Mahaleh, S. K. Sadrnezhaad, D. Hosseini, *Journal of Nanomaterials*, **1-4** (2008).

9. A. Aslania, V. Oroojpour, M. Fallahi, *Appl. Surf. Sci.*, **257**, 4056(2011).
10. Kh. S. Khashan, Gh. M. Sulaiman, F. A. K. A. Ameer, and G. Napolitano, *Pak. J. Pharm. Sci.*, **29** (2), 541 (2016).
11. M. A. Gondal, T. A. Saleh, Q. A. Drmosh, *Appl. Surf. Sci.*, **258**, 6982 (2012).
12. J. Hrenovic, J. Milenkovic, N. Daneu, R. M. Kepcija, N. Rajic, *Chemosphere*, **88**, 1103 (2012).
13. A. Azam, A. S. Ahmed, M. Oves, M.S. Khan, A. Memic, *Int. J. Nanomed.*, **7**, 3527 (2012).1
14. T. F. Jiao, J. Zh, J. X. Zhou, L. H. Gao, Y. Y. Xing, X. H. Li, *Iranian Polymer Journal*, **20** (2), 123 (2011).
15. K. S. V. Krishna Rao, K. Madhusudana Rao, P. V. Nagendra Kumar, I.-D. Chung, *Iranian Polym. J.*, **19**, 265 (2010).
16. E. Ispir, *Dyes Pigments*, **82**, 13 (2009).
17. N. Velmurugan, G. G. Kumar, S. S. Han, K. S. Nahm, Y. S. Lee, *Iran Polym. J.*, **18**, 383 (2009).
18. B. Dojer, A. Pevec, P. Šegedin, *Inorg. Chim. Acta*, **363**, 1343 (2010).
19. L. Li, F. Yuan, *Synth. React. Inorg., Metal-Org., Nano-Metal Chem.*, **42**, 205 (2012).
20. C. Yenikaya, M. Poyraz, M. Sarı, F. Demirci, H. Ilkimen, O. Büyükgüngör, *Polyhedron* **28**, 3526 (2009).
21. A. N. Emam, S. A. Loutfy, A. A. Mostafa, H. M. Awad, M. B. Mohamed, *RSC Adv.*, **7**, 23502 (2017).
22. A. K. E. El-Ansary, N. A. Mohamed, Kh. O. Mohamed, H. M. W. Abd-Elfattah, M. El-Manawaty, *Research Journal of Pharmaceutical, Biological and Chemical Sciences*, **6** (4), 1745 (2015).
23. M. R. Kasaai, *Carbohydr. Polym.*, **71**, 497 (2008).
24. E. R. Welsh, C. L. Schauer, S. B. Qadri, R. R. Price, *Biomacromolecules*, **3**, 1370 (2002).
25. C. Yenikaya, M. Poyraz, M. Sarı, F. Demirci, H. Ilkimen, O. Büyükgüngör, *Polyhedron*, **28**, 3526 (2009).
26. J. Kim, D. Kim, B. Veriansyah, J. W. Kang, J. D. Kim, *Mater. Lett.*, **63**, 1880 (2009).
27. D. L. Wilson, D. R. Wirz, G. H. Schenk, *Anal. Chem.*, **45**, 1447 (1973).
28. O. J. Olaniyan, E. O. Dare, O. R. Adetunji, O. O. Adedeji, Sh. O. Ogungbesan, *Nano Hybrids and Composites*, **11**, 22 (2016).
29. M. El-Kemary, N. Nagy, I. El-Mehasseb, *Materials Science in Semiconductor Processing*, **16**, 1747 (2013).
30. M. Fang, J. H. Chen, X. L. Xu, P. H. Yang, H. F. Hildebrand, *International Journal of Antimicrobial Agents*, **27**(6), 513 (2006).
31. C. Karunakaran, P. Gomathisankar, G. Manikandan, *Materials Chemistry and Physics*, **123**(2), 585 (2010).
32. L. Umaralikhana, M. J. M. Jaffar, *Journal of Advanced Applied Scientific Research*, **1-4** (8), 24 (2016).
33. P. Hosseinkhani, A. M. Zand, S. Imani, M. Rezayi, S. R. Zarchi, *International Journal of Nano Dimension*, **1**(4), 279 (2011).